Compression moulding of composites with hybrid fibre architectures

D. M. Corbridge, L. T. Harper*, D. S. A. De Focatiis and N. A. Warrior
Composites Research Group, Faculty of Engineering,
University of Nottingham, UK, NG7 2RD
*lee.harper@nottingham.ac.uk

Abstract

Advanced Sheet Moulding Compounds (ASMC) and unidirectional (UD) prepregs have been co-compression moulded to form a hybrid composite material. In-mould flow influences the UD fibre architecture in two ways. When UD fibres are aligned transversely to the ASMC flow direction, shearing occurs which causes local changes in fibre volume fraction and fibre waviness. When the UD fibres are aligned with the ASMC flow direction, ply migration takes place. In general, the composite stiffness follows a rule of mixtures relationship, with the stiffness proportional to the UD fibre content.

A grid analysis method has been developed to quantify distortion in the UD plies. Staging the resin to 50% cure was shown to reduce ply distortion during moulding, whilst maintaining suitable inter-laminar shear strength. Adding an interfacial prepreg ply between the reinforcing UD fibres and the ASMC charge successfully prevented distortion in the UD fibres, avoiding shear thinning and fibre migration.

Keywords

Compression moulding, sheet moulding compound, Carbon fibre

1 Introduction

Advanced sheet moulding compounds (ASMC) are typically formed from chips of unidirectional (UD) prepreg (50 mm × 8 mm) which are randomly dispersed and pressed together to form a sheet material [1]. Efficient packing of the filaments within the UD chips enables fibre volume fractions of up to 60% to be achieved [2], which are far higher than those of conventional glass fibre SMCs (typically 10-20% [3]), with tensile stiffness and strength of 30-35 GPa and 250-300 MPa respectively [4]. Whilst these properties are typically lower than those of continuous carbon fibre composites, discontinuous random fibre architecture have been shown to be relatively insensitive to notches and defects [5, 6], as stress concentrations present at the bundle ends are often larger than geometrical stress concentrations resulting from the notch [7].

The addition of local continuous UD fibre plies to the discontinuous ASMC architecture has the potential to enhance the mechanical performance of these materials, making them suitable for structural applications. Carbon prepregs have traditionally been formulated for autoclave use, but recent developments in fast curing resins (<5 minutes) have enabled them to be used to produce components with relatively simple geometries by compression moulding [8]. This paper investigates the possibility of co-moulding ASMCs and UD prepregs together to form a hybrid material. This creates an opportunity for producing highly optimised fibre architectures, by aligning continuous UD fibres with principal stresses for the primary load case and exploiting discontinuous fibres for secondary stress states such as off-axis loading, or for damage tolerance requirements. The continuous fibre plies will be cut as simple, nestable shapes to maximise material utilisation and minimise charge preparation times. The discontinuous fibres will flow during the compression moulding

stage, filling complex regions of the component and encapsulating fasteners. Co-moulding of these materials brings together the advantages of the two different fibre architectures to produce load-bearing and autoclave-quality parts, using an out-of-autoclave process [9]. This is of particular interest for automotive components, which are typically driven by stiffness rather than strength. The addition of the UD plies will significantly improve the tensile stiffness, but improvements in tensile strength are limited due to stress concentrations in the ASMC [10]. The UD fibres are more effective in bending however, as they are typically located at the surface of the plaque and therefore further from the neutral axis. This could potentially change the failure mode, which is particularly important in, for example, energy absorption studies for crashworthiness.

Material flow during compression moulding of hybrid fibre architectures can result in distortion in the continuous fibre reinforcement [8, 11], in the form of fibre waviness, ply splitting or ply migration. Mallick [12] produced hybrid architectures from glass SMCs and continuous glass fibre plies and demonstrated the reduction in properties as the initial charge size decreased. This was attributed to an increase in fibre waviness of the continuous fibres with increasing flow. This has also been observed for hybrid thermoplastic compounds, as the discontinuous fibres tend to drag, penetrate or disrupt the continuous fibre reinforcement. A study by Hangs et al. [11] suggests that the quality of the continuous fibre plies is strongly controlled by charge design and charge location within the tool. An initial overlap of the two materials was seen to significantly reduce the risk of distortion to the continuous fibres.

Discontinuous ASMCs tend to employ high viscosity epoxy matrices to avoid fibre/matrix separation during moulding [13] which can limit the amount of overall charge flow due to

higher friction levels at the mould-composite interface [14]. Initial tool coverage for the ASMC therefore tends to be high (80-90%) in order to minimise the required flow distance, and complex features such as ribs and stiffeners have to be processed at high pressures (>100 bar) to avoid incomplete filling. The high friction levels and viscous matrix therefore further increase the possibility of distortion in the continuous fibre plies. One possible solution is to increase the viscosity of the continuous UD reinforcement. Many high performance epoxies are formulated as B-staged systems, where the reaction between the resin and the curing agent is incomplete after mixing. Chemical or thermal B-staging can be used to partially cure the epoxy in order to increase the viscosity, but with full cross-linking only taking place when the system is reheated at a higher temperature. B-staging can therefore potentially be used to control the viscosity of the matrix in the UD plies, to prevent distortion during the over-moulding of the discontinuous ASMC.

The first objective of this paper is to investigate the performance gains for an ASMC when combined with continuous fibre reinforcement, for a charge design where high levels of flow are anticipated. A quantitative analysis of the distortion of the continuous fibres is carried out using a grid strain method and expressed in terms of UD fibre translations and rotations. The second objective is to evaluate the potential for using resin staging to prevent distortion of the continuous fibre plies. The grid strain analysis is used to compare the levels of distortion against the non-staged benchmark, and short beam shear tests are performed to understand the influence of staging on the inter-laminar shear strength. The third and final objective is to investigate how charge design can be used to control and mitigate distortion of the continuous fibres.

2 Experimental methodology

2.1 Materials

The ASMC used in this study was HexMC®/C/2000/M77, supplied by Hexcel, Duxford, UK. This is a carbon fibre sheet moulding compound with an areal density of 2000 gsm (approximate, as supplied), consisting of carbon fibres (57% fibre volume fraction, V_f) impregnated with M77 epoxy resin. M77 is a fast curing epoxy (2 minutes at 150°C) that has been specifically developed for compression moulding.

HexPly® UD prepreg M77/38%/UD300/SGL-50K, which uses the same epoxy resin, was also supplied by Hexcel. This material is manufactured using 50K high strength carbon fibres supplied by SGL Group, with a fibre areal density of 300 gsm. The final prepreg areal density is 484 gsm, which equates to a V_f of 53% (as supplied).

Table 1 gives an overview of the construction of the hybrid plaques produced and the notation used to describe each charge. For example, UD3/90°/SMC2/60% consists of three plies of UD prepreg (UD3) with the fibres aligned at 90° to the flow direction, placed on top of two plies of HexMC (SMC2). Both components have 60% areal coverage of the tool surface.

2.2 Resin staging

An Anton Paar Modulus Compact Rheometer MCR 302, fitted with a CTD 450 convection temperature chamber, was used to determine the shear storage modulus as a function of temperature and time. Samples of M77 resin were unavailable for this study and resin could not be reliably extracted from the prepreg, therefore Ø25 mm discs of UD prepreg were cut using a punch. Specimens were placed between 25 mm parallel plates in the rheometer, and

an oscillation with an apparent strain amplitude of 0.1% (based on the nominal thickness) at a frequency of 10 Hz was imposed, together with a normal force of 1 N. The temperature was held at 20 °C for 1 minute before ramping up to 90 °C at a rate of 5 °C/min. This ramp rate was selected to represent the heating rate achieved in the oven, which was used for staging the larger prepreg specimens. The temperature was held at 90 °C for 100 minutes, until the prepreg was fully cured (i.e. the storage modulus settled to a constant value). Five specimens were tested, and the average normalised storage modulus is presented as a function of time in Figure 2. Some inter-specimen variability was observed, and can be attributed to inconsistent resin/fibre ratios in the small prepreg specimens, and fibre misalignment. Five staging times corresponding to increments in the average normalised storage modulus of 25% were determined from the data, which are summarised in Table 1. These times were used to stage the UD plies in the hybrid architecture study, using a Heraeus Function Line oven at a set-point of 90°C.

2.3 Moulding

2.3.1 Compression moulding

Compression moulding was performed in a 405 mm × 405 mm flat plaque tool mounted in a Daniels upstroke press. The maximum achievable pressure over the tool area was 85 bar. The tool had an 18 mm radius in the four corners and a central 100 mm × 100 mm ejection plate to aid part removal. Hard stops were not used in order to ensure a known, uniform pressure was applied to the charge. The thickness of the final plaque was therefore determined by accurate control of the initial charge volume (determined from the mass and density). Two symmetric charges were placed in the tool simultaneously to prevent the floating press platens from misaligning during compression, as shown in Figure 1. Charges

were positioned along opposite edges of the tool to encourage a one-dimensional flow scenario, initially covering 60% of the tool area.

Since the recommended moulding pressure for the UD material (8 bar) was insufficient to cause flow in the ASMC, the recommended cure cycle for the ASMC material was adopted for manufacturing the hybrid plaques. Plaques were moulded isothermally at 130 °C for 8 minutes at a pressure of 84 bar. Faster cure times were available (2 mins at 150 °C), but the chosen cycle provided sufficient time to position the charge and close the tool in the laboratory setup (at a closure speed of 150 mm/min) before gelation.

2.3.2 Out-of-autoclave moulding

An out-of-autoclave (OOA) manufacturing method was used to produce specimens to evaluate the quality of the interface between staged and non-staged UD prepregs. This manufacturing route was chosen to avoid material flow, in order to isolate the effects of resin staging from the influence of the fibre architecture. Typically, three unstaged UD plies were stacked on top of three staged UD plies and then assembled on a 5 mm thick aluminium plate. Cork strips were positioned around the perimeter to avoid excessive resin bleed during curing. A 5 mm thick aluminium caul plate was then added on top of the laminate to ensure a uniform surface finish, before the whole assembly was vacuum-bagged and then cured in a hot-air oven at 130°C for 1 hour. A full vacuum was maintained throughout the curing process, including the cool down period to ambient.

Selected laminates were debulked during the layup process before moulding. For a debulked laminate, three plies of the as-received UD were stacked together and debulked for 15 minutes at a minimum vacuum pressure of 960 mbar, at ambient temperature,

before being placed in the line oven to be staged at 90°C. These staged plies were then removed from the oven and cooled. Three unstaged plies were then subsequently placed on top of the three staged plies to create the laminate described above, which were then debulked under vacuum for a further 15 minutes, before the entire arrangement was placed in the oven for 1 hour at 130 °C for the final cure cycle.

2.4 Mechanical testing

Four-point flexural testing was conducted according to BS EN ISO 14125:1998+A1:2011. Testing was carried out within the elastic limit, at strains of up to 0.2%, which enabled multiple flexural tests to be performed along the length of each specimen without inducing damage. Figure 3 confirms that this strain threshold is within the elastic region of the stress/strain curves for all of the material scenarios tested. This approach enabled the local stiffness variation to be investigated, which is reported to vary by up to ±20% for random discontinuous moulding compounds [1]. A fixed span of 75 mm was used, which equated to a span-to-thickness ratio of 37.5:1. This ratio was used to minimise through-thickness shear effects [15], and enabled 6 tests per specimen to be conducted (25 mm between measurement points). The accuracy of the measurement of the central deflection of the specimen was improved by using a linear voltage displacement transducer at the centre of the specimen.

Short beam shear testing was conducted according to BS EN ISO 14130:1998 to measure the apparent inter-laminar shear strength (ILSS). A 2 mm plaque thickness was not always

possible due to the discrete thickness constraints of the laminar plies. An appropriate thickness correction factor was used to calculate the ILSS as stated in the standard.

All mechanical tests were performed at room temperature at a speed of 1 mm/min on an Instron 5578 universal testing machine.

2.5 Fibre volume fraction

A Mettler Toledo XS105 Dual Range scale (readability of 0.01 mg at a maximum capacity of 41.0 g, with a repeatability of 0.02 mg) was used with an Archimedes density fixture, in order to determine the density of each sample from measurements of the weight in water and air. A wetting agent was applied to the surface of the specimen (Pervitro 75%) to prevent bubbles occurring when the specimen was lowered into de-ionised water. Prior to testing, carbon fibre specimens were deburred with P600 abrasive paper to remove splintering from the edges caused by cutting. For the determination of the fibre volume fraction (V_f), densities of 1.22 g/cm^3 and 1.80 g/cm^3 were assumed for the resin and carbon fibres respectively, taken from the manufacturer's data sheets.

This method was chosen over alternatives such as acid digestion, because it was fast and simple to perform for the large volume of specimens. The local volume fraction was measured at the same location as each of the local stiffness measurements on the four-point bend specimens. Six Vf measurements were taken for each four point bend specimen, with up to 72 individual measurements taken per plaque.

3 Fibre distortion measurement

3.1 Photogrammetry

Photogrammetry was used to quantify distortion in the UD plies, using a grid analysis technique. A 1.2 mm wide yellow Artline 440XF paint marker (Shachitata Ltd) was used with a transparent plastic template to draw a series of parallel grid lines at 20 mm spacing in two perpendicular directions on the surface of the top UD ply prior to moulding. A Xerox 7556 flatbed scanner was used to digitise the grid before and after moulding, which eliminated the need to correct for perspective. The micrograph shown in Figure 4(a) demonstrates that applying the grid to the top ply is an effective way to capture the representative flow behaviour of all of the UD plies. The plies tend to migrate and distort in the same way through the thickness when the fibres are aligned in the same direction. Figure 4(b) shows a micrograph from the surface of the UD3/0°/60% sample after moulding, which indicates that the yellow paint encapsulates the surface filaments, but does not penetrate further through the thickness of the laminate. Figure 4(c) demonstrates that the yellow paint is representative of the fibre behaviour rather than the resin behaviour, as resin migration has clearly occurred (see bottom of image) but the grid is undistorted since the fibres did not move.

3.2 Grid analysis

The scanned images of the grids were imported into Matlab® 2014b to determine the intersection points using the Image Processing Toolbox. A binary image of each plaque was created by setting a threshold brightness value, as shown in Figure 5(a). The lighting from

the scanned images is highly repeatable, however the level of material flow affects the quality of the grid and therefore the threshold value was adjusted accordingly each time.

The width of the pen lines makes it difficult to precisely determine the intersection point. Skeletonisation (an inbuilt Matlab function) was used to erode the binary image to create a single pixel width line by removing pixels equally from each side of the drawn line. The intersection points are plotted for UD3/90°/SMC2/60% in Figure 5(b), excluding any intersections around the perimeter of the grid.

Intersections were determined from the grids drawn on the original charge packs and the corresponding moulded plaques to enable the relative displacements to be calculated. The intersection points were used to define 4-noded linear elements to enable a displacement field to be calculated, using an approach similar to that of Buerzle et al.[16]. Basic deformation modes of the UD material can be determined by considering the translation, rotation and elongation of the grid elements. Elongation in this case, ε, is defined as the relative extension of grid elements arising from flow of the material, rather than stretch of the fibres during moulding. The rotations and elongations in the direction of flow are plotted for UD3/90°/SMC2/60%/S25% in Figure 5(c) and Figure 5(d) respectively.

4 Results and discussion

4.1 Effect of hybridisation

Non-hybrid plaques were initially compression moulded to give suitable baselines for comparison against the hybrid architecture plaques (see plaques 1.1 – 1.5 in Table 1). The flexural stiffness values are summarised in Figure 6 for two test directions, where 0° corresponds to the flow direction. Two ASMC plaques were manufactured with different

charge coverage levels (100% and 60%) to investigate the influence of in-mould flow. The normalised flexural stiffness of the net-shaped charge (SMC2/100%) was found to be (33 ± 1.2) GPa (95% confidence interval) for both test orientations. The flexural stiffness of the SMC2/60% plaque increased to (47 ± 2.6) GPa in the 0° test direction due to flow-induced fibre alignment, which can be observed on the surface of the plaque. The stiffness in the 90° test direction correspondingly reduced to (23 ± 2.3) GPa.

A similar study was performed for the UD prepreg and the average normalised stiffness of the net-shaped plaque (UD3/0°/100%) was (119 ± 1.87) GPa. When the fibres were aligned in the flow direction, the normalised stiffness for the 60% coverage plaque was similar, at (117 ± 1.1) GPa, as the fibres did not distort during compression. Figure 7(a) indicates that the UD fibres for the UD3/0°/60% plaque remained straight and the ply stack did not migrate during moulding. There was noticeable resin bleed at the fibre ends, which resulted in some resin loss through the flash gap in the tool. This is reflected in the local V_f measurements, which range from 67-73% and are generally higher at the fibre ends according to Figure 7(d). Consequently the local flexural modulus was directly proportional to the local V_f, as there was no local change in fibre orientation.

The UD fibres were significantly influenced by resin flow when oriented transversely to the flow direction (UD3/90°/60%). The grid in Figure 7(a) shows that the charge extends uniformly within the tool, as each grid element travels a progressively larger distance. However, Figure 7(b) indicates that the edges of the UD3/90°/60% charge have been subjected to greater levels of rotation, which can be attributed to frictional effects along the vertical tool walls. The local flexural stiffness is therefore dependent on both the fibre orientation and the V_f for this scenario. The average normalised flexural stiffness for

UD3/90°/60% in the fibre direction (transverse to the flow direction) was (105 ± 2.2) GPa, which is 10% lower than that of UD3/0°/60%. Local variability in the flexural stiffness is also higher for the UD3/90°/60% than the UD3/0°/60% according to Figure 7(d), which ranged from 91 GPa to 123 GPa (before normalisation to 55% V_f). This can be attributed to greater levels of fibre rotation and transverse shearing in the UD ply, as is clearly visible from the grid analysis.

Two hybrid architecture plaques were moulded as part of this study to investigate the combined effects of local SMC flow and the UD ply orientation relative to the global flow direction. Figure 8 shows a summary of the distortion observed in the UD plies for both UD3/0°/SMC2/60% and UD3/90°/SMC2/60%. There are much greater levels of distortion in the UD plies of UD3/0°/SMC2/60%, compared to the 0° UD plies in Figure 7. The UD plies in UD3/0°/SMC2/60% have all migrated away from the top tool edge as the SMC material has flowed towards the centre of the tool. The element elongation plot in Figure 8(a) indicates that the UD elements in UD3/0°/SMC2/60% have elongated very little, but large element rotations are observed at the side walls due to the friction. The behaviour of the UD plies in UD3/90°/SMC2/60% is similar to the behaviour observed for the SMC material with 60% charge coverage. The dominant distortion mechanism is flow-induced shearing of the material. The original grid lines remain in contact with the boundary of the plaque, therefore the UD plies do not appear to have migrated globally due to the flow. The grid has deformed locally due to the heterogeneous flow of the underlying SMC and there are no distinguishable patterns for the elongation or rotation of the elements.

The average normalised flexural stiffness values for UD3/0°/SMC2/60% and UD3/90°/SMC2/60% follow a rule of mixtures (ROM) relationship and are between the

stiffness values of the SMC and the UD, as shown in Figure 6. The normalised experimental stiffness for UD3/0°/SMC2/60% is (74 ± 2.8) GPa, compared to 75 GPa from the ROM (using the individual stiffness values from UD3/0°/60% and SMC2/60%). The normalised experimental stiffness for UD3/90°/SMC2/60% is (52 ± 4.9) GPa , compared to 46 GPa from the ROM.

4.2 Effect of resin staging

Resin staging was investigated as a possible method for controlling the shape and position of UD prepreg plies during compression moulding of hybrid laminates. All charge packs were initially 405 mm × 122 mm and covered 60% of the tool area, with three UD plies on top of two SMC plies (based on UD3/90°/SMC2/60%). The UD fibres were oriented transversely to the flow direction, as this scenario produced the most disruptive flow patern for the UD material in terms of element elongation (fibre shearing) according to Figure 8. Figure 9 shows grid analyses illustrating the effect of increasing levels of staging according to the staging times presented in Table 1. Table 2 summarises the grid data in terms of element elongation, translation and rotation, in order to compare the staged plaques against the benchmarks.

Figure 9 indicates that the flow front of the UD material is approximately uniform, with little migration of the UD plies. For plaques with no/low levels of staging, distortion occurs due to resin flow, resulting in grid elongation. The two UD ply stacks for the 0% staged plaque (UD3/90°/SMC2/60%) flowed a distance of 80mm (from each side) and met in the centre, creating a weld line. The average element elongation in the flow direction (y-direction) for this plaque was 77% according to Table 1, and may have been greater had the two charges

not met. The maximum elongation in the flow direction was 186%, and can be observed in the top left hand corner of the unstaged plaque in Figure 9.

Increasing the level of staging to 25% reduces the flow-induced distortion in the UD plies considerably. The mean and maximum elongation values are reduced to 20% and 51% respectively. It can be seen from Figure 9 that the UD plies no longer meet in the centre, despite the SMC creating a central weld line. Similar flow characteristics are observed for the 50% staged plaque, with comparable elongation values reported in Table 2.

Further reductions in distortion are possible if the staging level is increased to 75% (10% mean elongation). The 75% staged UD material limited the flow of the SMC, and this was the only hybrid scenario where an incomplete weld line was observed in Figure 9. However, this level of staging severly affects the interfacial properties. Figure 10 shows interlaminar shear strength (ILSS) values for the UD plies as a function of the level of staging. In general there is a linear reduction in ILSS with increasing staging for the non-debulked plaques. The ILSS for the 75% staged plaque is lower than the apparent ILSS reported for the SMC material, which was considered to be the acceptable threshold for this study. Figure 11 shows that the interlaminar fracture sites are all concentrated between the staged prepreg plies, indicating that the interfacial adhesion is lower than between the non-staged plies. According to Figure 10, debulking the UD plies during the staging process increases the ILSS by approximately 35% for the 75% staged plaque, making it higher than the SMC threshold. Void measurements by optical microscopy indicated that the average void content was reduced from 3% by volume to 1.5% when debulking was performed. According to Figure 9, debulking also influences the flow characteristics of the UD, reducing the amount of distortion (UD3/90°/SMC2/60%/s50/D shown) compared to a non-debulked plaque with the

same level of staging. This can be attributed to improved nesting of the fibres and greater friction between the plies. The same effect may be achievable by cold-pressing the UD plies before compression moulding hybrid parts.

Whilst debulking had a significant effect on the flow behaviour of the UD material in the hybrid plaques, it is not considered to be a viable solution for controlling distortion in high volume applications due to the required 15 minute cycle time.Resin staging had a dramatic effect on the flow behaviour of the UD plies, but this consequently had adetrimental effect on the interlaminar properties.

4.3 Effect of charge design

The following section investigates controlling the distortion in the UD plies by changing the charge construction. Figure 7 and Figure 8 demonstrate that the flow characteristics for the UD plies are dependent on the orientation of the fibres relative to the flow direction, with greater distortion occuring when the fibres are aligned transversly to the flow direction. A study was conducted to investigate the influence of a cross-ply UD architecture (fibres aligned in both 0° and 90°) to control the distortion of the primary reinforcement. A hybrid plaque was manufactured with the ASMC and UD fibres oriented in the two principal directions. Two UD plies were orientated transverse to the flow direction (90°). The third UD ply was positioned between the two 90° plies and the ASMC material and the fibres were orientated in the flow direction (0°). This 0° ply acted as an interfacial layer to help prevent distortion in the 90° UD plies, whilst aiming to maintain a high level of interfacial adhesion by avoiding the need for high levels of staging. A summary of the charge construction for Plaque 3.1 is shown in Table 1, which should be compared to Plaque 2.3 from the staging study (UD3/90°/SMC2/60%/S50%).

Figure 12 shows that the cross-ply layup of the UD layers reduces the distortion in the transverse plies compared to the UD3/90°/SMC2/60%/S50% benchmark. According to Table 2, the maximum element elongation in the y-direction is 7%, which is comparable to a hybrid plaque manufactured with three plies of UD aligned in the flow direction (UD3/0°/SMC2/60%/S50% in Table 2). The resulting flow behaviour of the UD is similar in both directions, as the elongation values are similar in both the x and y directions. Adding an interfacial UD ply with fibres oriented in the flow direction has a similar effect to debulking the UD plies at 50% staging, or staging the resin to 75%. It is possible that an increasing number of transverse plies will be required to control the flow behaviour of the longitudinal plies as the overall number of UD plies increases. It is interesting to note that the interfacial ply has not had a dramatic influence on the overall stiffness of the laminate. As reported in Table 2, substituting one of the 90° plies with a 0° interfacial ply only reduces the average flexural stiffness from (47.8 ± 2.1) GPa (UD3/90°/SMC2/60%/S50%) to (44.1 ± 1.9) GPa (UD3/90°,90°,0°/SMC2/60%/S50%). This emphasises the importance of charge design, as preserving the alignment of the UD fibres is critical for achieving worthwhile improvements in mechanical performance when hybridising UD fibres with SMC.

Figure 13 demonstrates the effectiveness of using a cross-ply UD layup to prevent distortion in a 2D flow scenario. The charge pack was placed centrally within the tool, with the SMC covering 60% by area and the UD 25%. Images of UD3/90°/SMC2/60%/S50% in Figure 13 show the flow behaviour of the UD material when all continuous fibres are aligned in the flow direction. The rotation and elongation of the central elements is small, but some distortion occurs along the sides of the UD plies due to the radial flow of the SMC. Images of UD3/90°,90°,0°/SMC2/60%/S50% in Figure 13 demonstrate the successful implementation

of the cross-ply design to prevent distortion in the UD plies. The average rotation and elongation are 1.1° and 0.1% respectively, which are comparable to the values reported for UD3/0°/60% in Table 2.

Only the in-plane distortion of the UD fibres was considered in the current work, but it is important to note that some of the UD/ASMC hybrid plaques exhibited out-of-plane warpage. Warpage is defined as the curvature and twist of initially flat parts, and is the result of a non–balanced stress distribution through the thickness of the laminate. Residual stresses are caused by the mismatch in coefficient of thermal expansion between the carbon fibre and epoxy matrix, and in this case, the magnitude of these stresses depends on the volume ratio of UD fibres to ASMC fibres, and the relative orientation of the UD plies. The warpage was more apparent for plaques containing UD plies orientated in the same direction, but there was a noticeable reduction in plaque curvature when the UD fibres were arranged in the cross-ply configuration. One potential solution is to create a more balanced laminate by adding UD fibres to both surfaces of the component, but this may not be practical for complex geometries. Out-of-plane warpage needs to be investigated further, but it may be insignificant if the ratio of UD/ASMC is low, the UD fibre plies are balanced or the UD fibres are localised over a small area.

5 Conclusions

The effect of compression moulding hybrid composites, by adding UD prepreg to a carbon fibre moulding compound, has been studied by measuring the local flexural stiffness and fibre volume fraction, and by a grid analysis. It has been shown that, in general, a rule of

mixtures relationship is observed for the stiffness, which is proportional to the quantity of UD material added. Flow of the SMC material influences the UD fibre architecture in two ways. Firstly, shearing of the UD ply occurs when the fibres are aligned transversely to the SMC flow direction, causing local changes in fibre volume fraction and fibre waviness. Secondly, ply migration occurs when the UD fibres are aligned with the SMC flow direction.

Advancing the degree of cure of the resin in the UD plies by staging has been demonstrated as an effective way to manufacture high quality hybrid architecture laminates by rapid compression moulding. Staging the resin to 50% cure was shown to adequately reduce ply distortion during moulding, whilst maintaining inter-laminar performance. Further reductions in ply distortion were achieved by debulking the plies before staging, but this route is impractical for high volume production. Adding an interfacial ply between the reinforcing UD fibres and the SMC charge successfully prevented distortion to the UD fibres, avoiding shear thinning and fibre migration in both 1D and 2D flow situations. The addition of the interfacial ply reduced the average flexural stiffness by just 8% compared to similar plaques where all UD fibres were aligned transverse to the flow direction. This highlights the significance of charge design and demonstrates how fibre orientation can be used to control the flow in UD plies when compression moulding hybrid architectures.

A grid analysis was presented to quantify the levels of distortion in the UD surface plies for different moulding scenarios. Microscopy was used to confirm that observations from the grid on the surface ply were representative of the behaviour of all UD fibre plies when oriented in the same direction. The grid data was used to study the influence of in-mould flow on the fibre orientation (element rotation), ply migration (element translation) and ply

deformation (element elongation). This grid data will be employed in future studies to develop predictive analytical models for the mechanical properties of such hybrids.

6 Acknowledgements

This work was funded by the Engineering and Physical Sciences Research Council [Grant number: EP/IO33513/1], through the ‘‘EPSRC Centre for Innovative Manufacturing in Composites’’.

7 References

1. P. Feraboli, E.P., T. Cleveland, B. P. Stickler, , *Modulus measurement for prepreg-based discontinuous carbon fibre/epoxy systems.* Journal of Composite Materials, 2009. **43**(19): p. 1947-1965.

2. McConnell, V.P., *New recipes for SMC innovation.* Reinforced Plastics, 2008. **52**(8): p. 34-39.

3. Cheon, J.-S. and Y.-T. Im, *Determination of Short Glass-Fiber Volume Fractions in Compression Molded Thermoset Composites—Experimental.* Journal of Composite Materials, 1999. **33**(6): p. 525-546.

4. Luchoo, R.H., L. T. Bond, M. D. Warrior, N. A., *Net shape spray deposition for compression moulding of discontinuous fibre composites for high performance applications.* Plastics Rubber and Composites, 2010. **39**(3-5): p. 216-231.

5. Feraboli P., C., Tyler, Ciccu, Marco, Stickler, Patrick, De Oto Luciano, *Defect and damage analysis of advanced discontinuous carbon/epoxy composite materials.* Composites Part A: Applied Science and Manufacturing, 2010. **41**(7): p. 888-901.

6. P. Feraboli, E.P., T. Cleveland, B. P. Stickler, , C. J. Halpin, *Notched behavior of prepreg-based discontinuous carbon fiber/epoxy systems.* Composites Part A: Applied Science and Manufacturing, 2009. **40**(3): p. 289-299.

7. Qian, C., Harper, L. T., Turner, T. A., Warrior, N. A., *Notched behaviour of discontinuous carbon fibre composites: Comparison with quasi-isotropic non-crimp fabric.* Composites Part A: Applied Science and Manufacturing, 2011. **42**(3): p. 293-302.

8. Akiyama, K. *Development of Prepreg Compression Moulding (PCM) technology*. in *SPE Automotive Composites Conference and Exhibition*. September 2011. Troy, Michigan.

9. Wulfsberg, J., Herrmann, Axel, Ziegmann, Gerhard, Lonsdorfer, Georg, Stöß, Nicole,Fette, Marc, *Combination of Carbon Fibre Sheet Moulding Compound and Prepreg Compression Moulding in Aerospace Industry.* Procedia Engineering, 2014. **81**: p. 1601-1607.

10. Johanson, K., L.T. Harper, M.S. Johnson, and N.A. Warrior, *Heterogeneity of discontinuous carbon fibre composites: Damage initiation captured by Digital Image Correlation.* Composites Part A: Applied Science and Manufacturing, 2015. **68**: p. 304-312.

11. Hangs, B., Jauch, M. R. R.,Henning, F., Grauer, D., Jespersen, S., Martsman, A. *Co-compression molding of tailored continuous-fiber inserts and inline-compounded long-fiber-thermoplastics*. in *Society of Plastics Engineers: Automotive Composites Conference and Exhibition 2012*. 2012. Troy, Michigan.

12. Mallick, P.K., *Effect of Fiber Misorientation on the Tensile Strength of Compression Molded Continuous Fiber Composites.* Polymer Composites, 1986(7(1)).

13. Dumont, P., Le Corre, Steven, Orgéas, Laurent, Favier, Denis, Gaborit, Cyril, Lory, Pierre, *Finite element implementation of a two-phase model for compression molding of composites.* Revue Européenne des Éléments, 2005. **14**(6-7): p. 885-902.

14. Guiraud, O.D., P. J. J. Orgéas, L. Favier, D., *Rheometry of compression moulded fibre-reinforced polymer composites: Rheology, compressibility, and friction forces with mould surfaces.* Composites Part A: Applied Science and Manufacturing, 2012. **43**(11): p. 2107-2119.

15. Harper, L.T., Ahmed, I., Felfel, R. M., Qian, C., *Finite element modelling of the flexural performance of resorbable phosphate glass fibre reinforced PLA composite bone plates.* Journal of the Mechanical Behavior of Biomedical Materials, 2012. **15**: p. 13-23.

16. Buerzle, W. and E. Mazza, *On the deformation behavior of human amnion.* Journal of Biomechanics, 2013. **46**(11): p. 1777-1783.

8 Figures

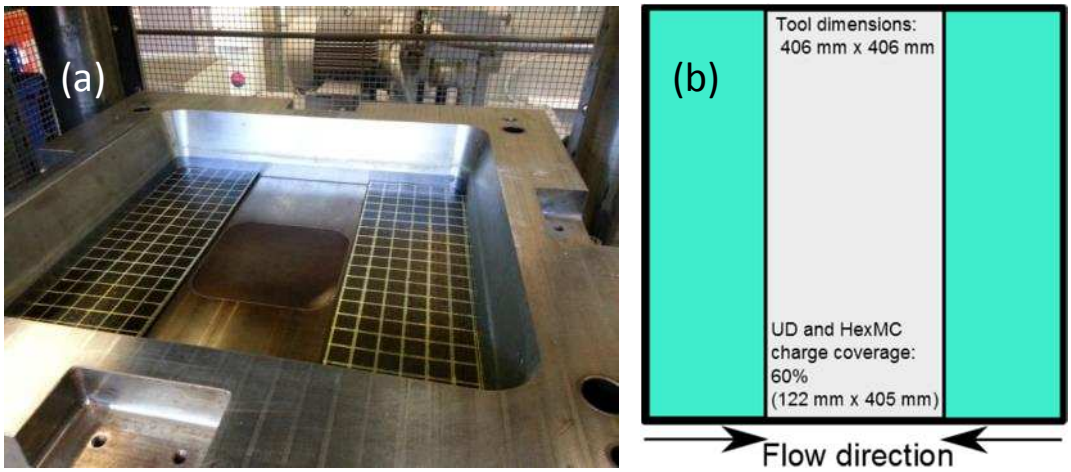

Figure 1: (a) Compression moulding tool showing charge location and the central ejector plate; (b) schematic diagram showing the charge dimensions for a typical 60% charge coverage.

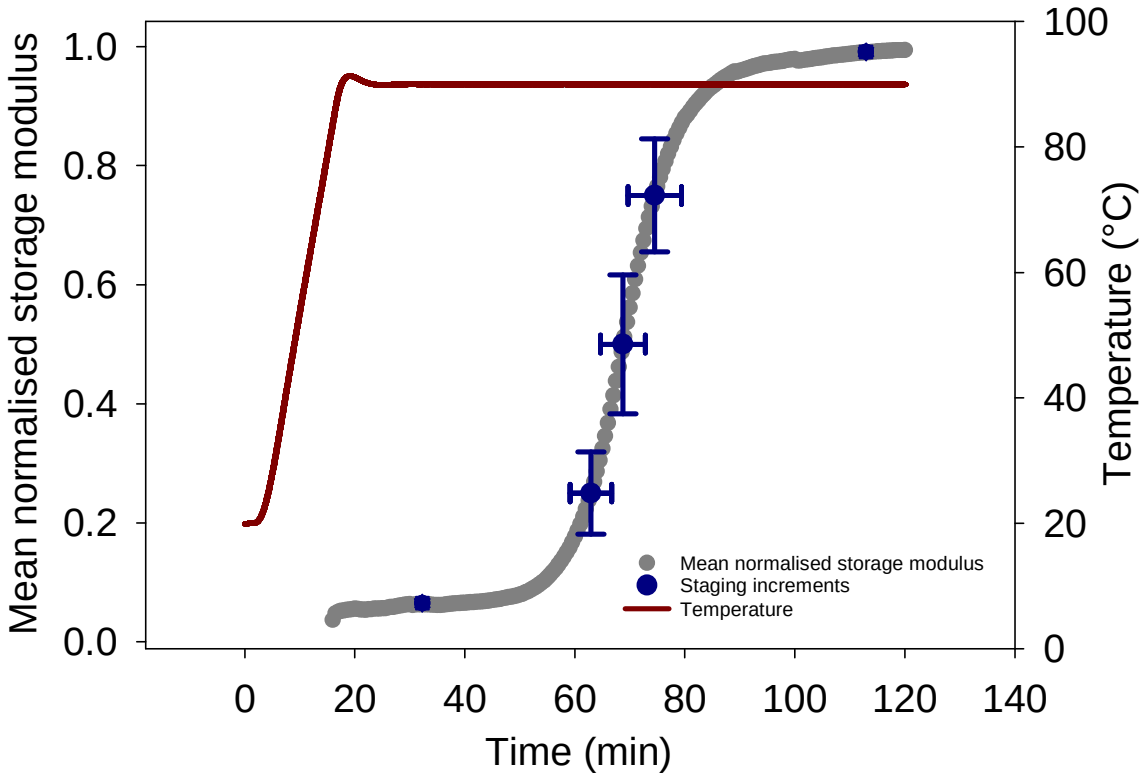

Figure 2: Mean normalised storage modulus measured using oscillatory parallel plate rheometry on UD prepreg circular disc specimens (left abscissa), heated from ambient to 90°C at a ramp rate of 5°C/min (right abscissa). 95% confidence intervals shown.

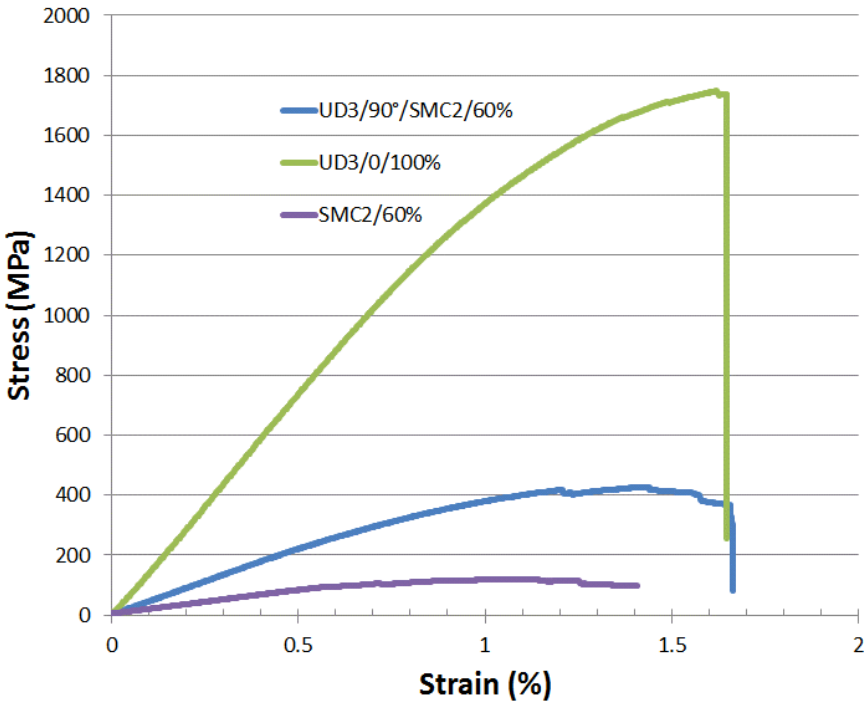

Figure 3: Stress/strain curves from four-point bending tests.

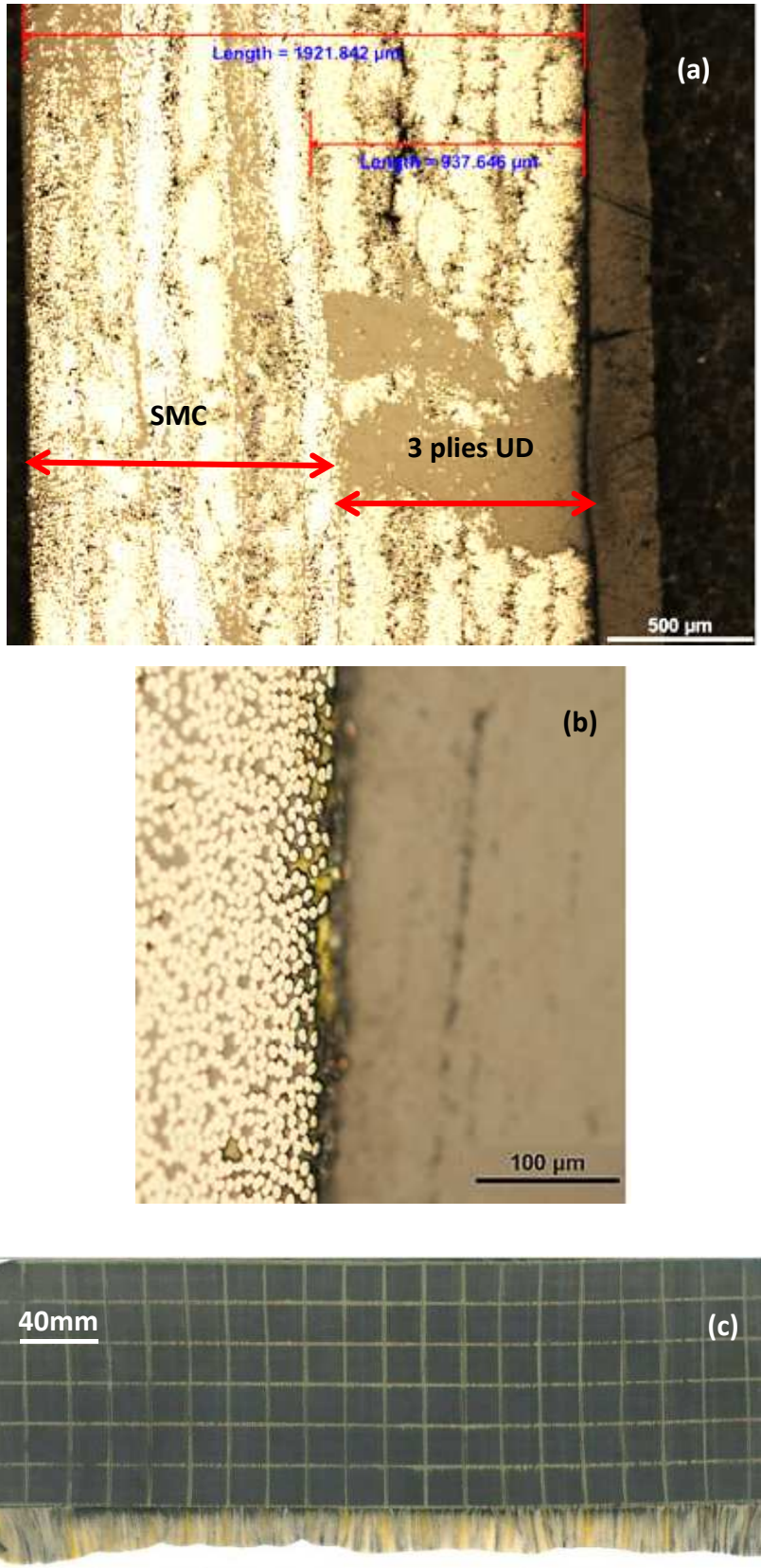

Figure 4: (a) Optical micrograph of a polished section from UD3/0°/SMC2/60% showing a split in the top three plies of UD. (b) Optical micrograph showing the distribution of the yellow paint marker used to define the grid for the photogrammetry study. (c) Surface scan of UD3/0°/60% showing migration of resin.

(a)

(b)

(c)

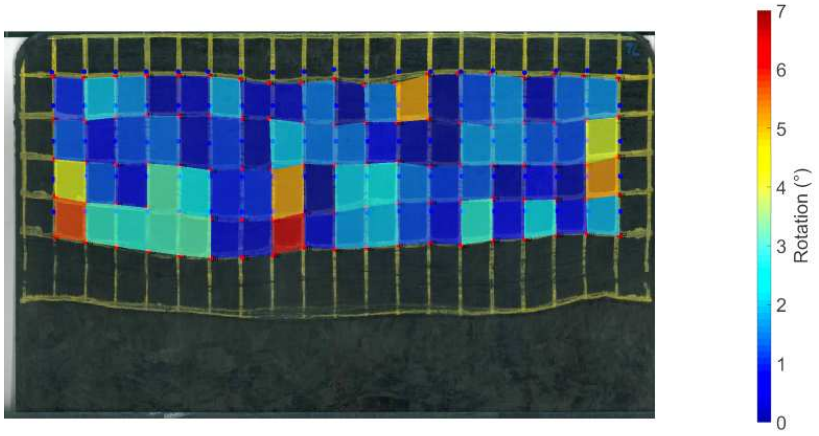

(d)

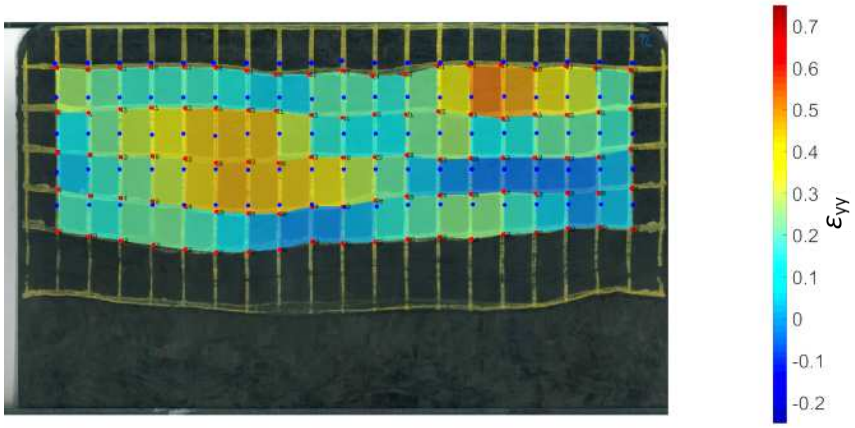

Figure 5: (a) Binary image of UD3/90°/SMC2/60%/S25%; (b) grid intersection points identified by Matlab code; (c) absolute rotation in degrees; (d) translation in the y-direction (ε_{yy})

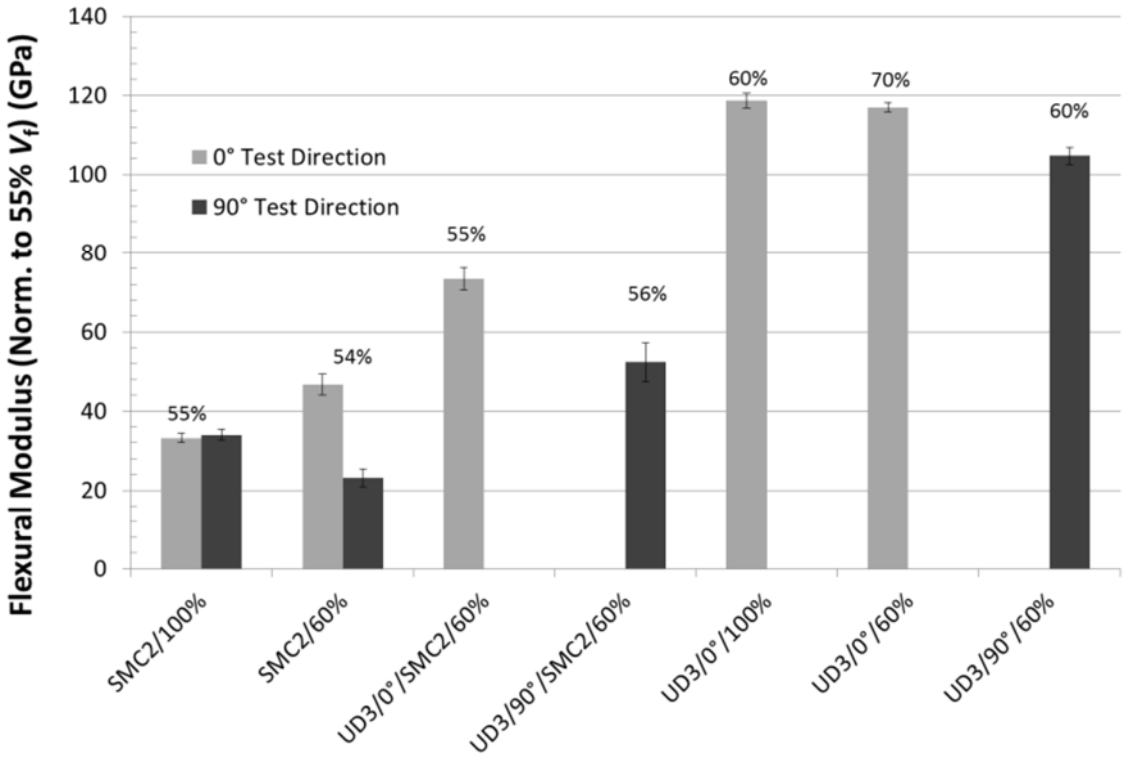

Figure 6: Average measurements of flexural modulus of hybridisation benchmark plaques, normalised to a fibre volume fraction of 55%. 95% confidence interval bars shown. The as-moulded fibre volume fractions are shown as percentages above the bars. Flow occurs in the 0^o test direction.

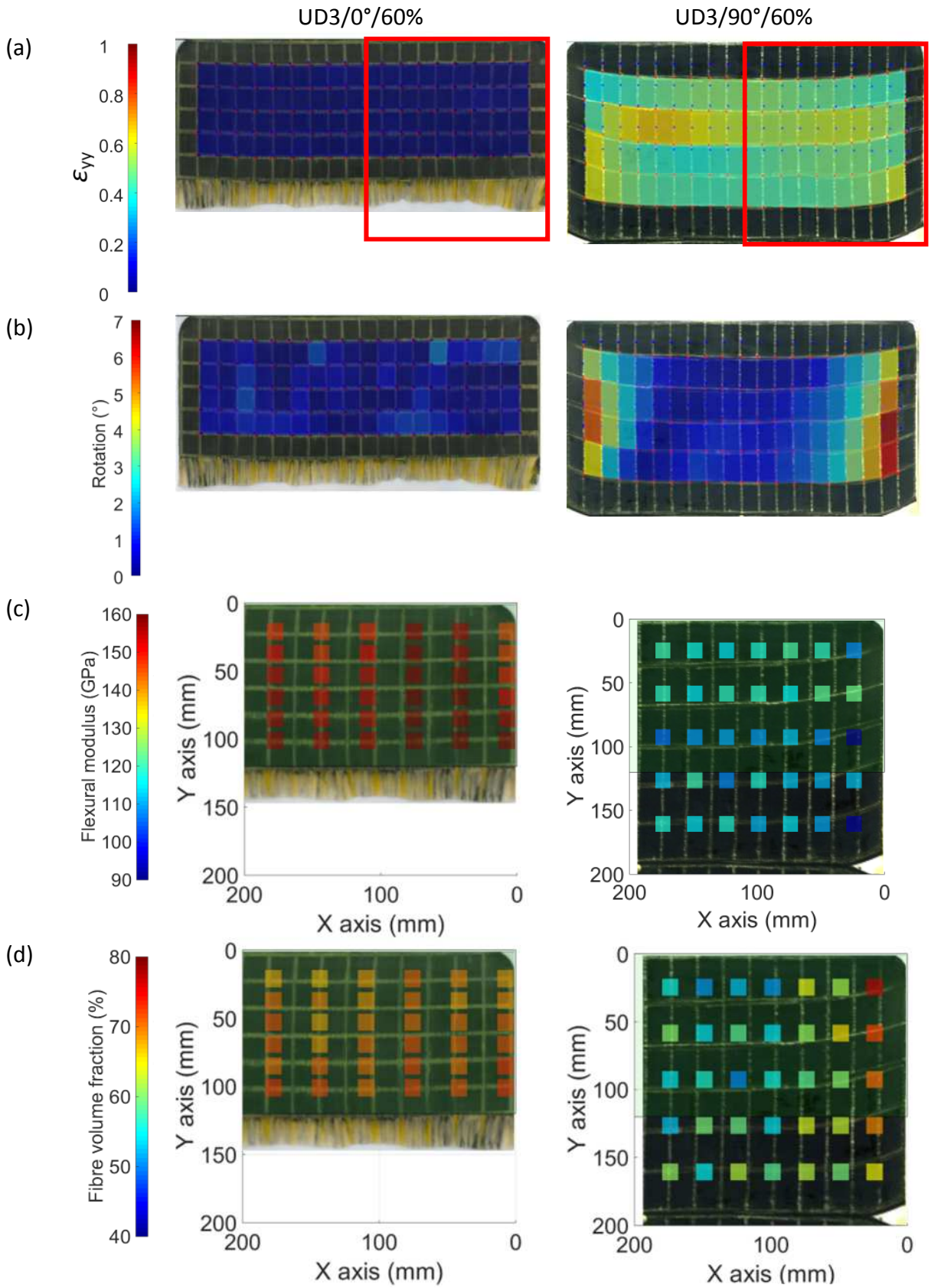

Figure 7: (a) Grid elongation, (b) grid rotation, (c) local flexural modulus and (d) local fibre volume fraction measurements for UD3/0°/60% and UD3/90°/60% hybrids. In (a), the red square indicates the location of modulus and volume fraction measurements.

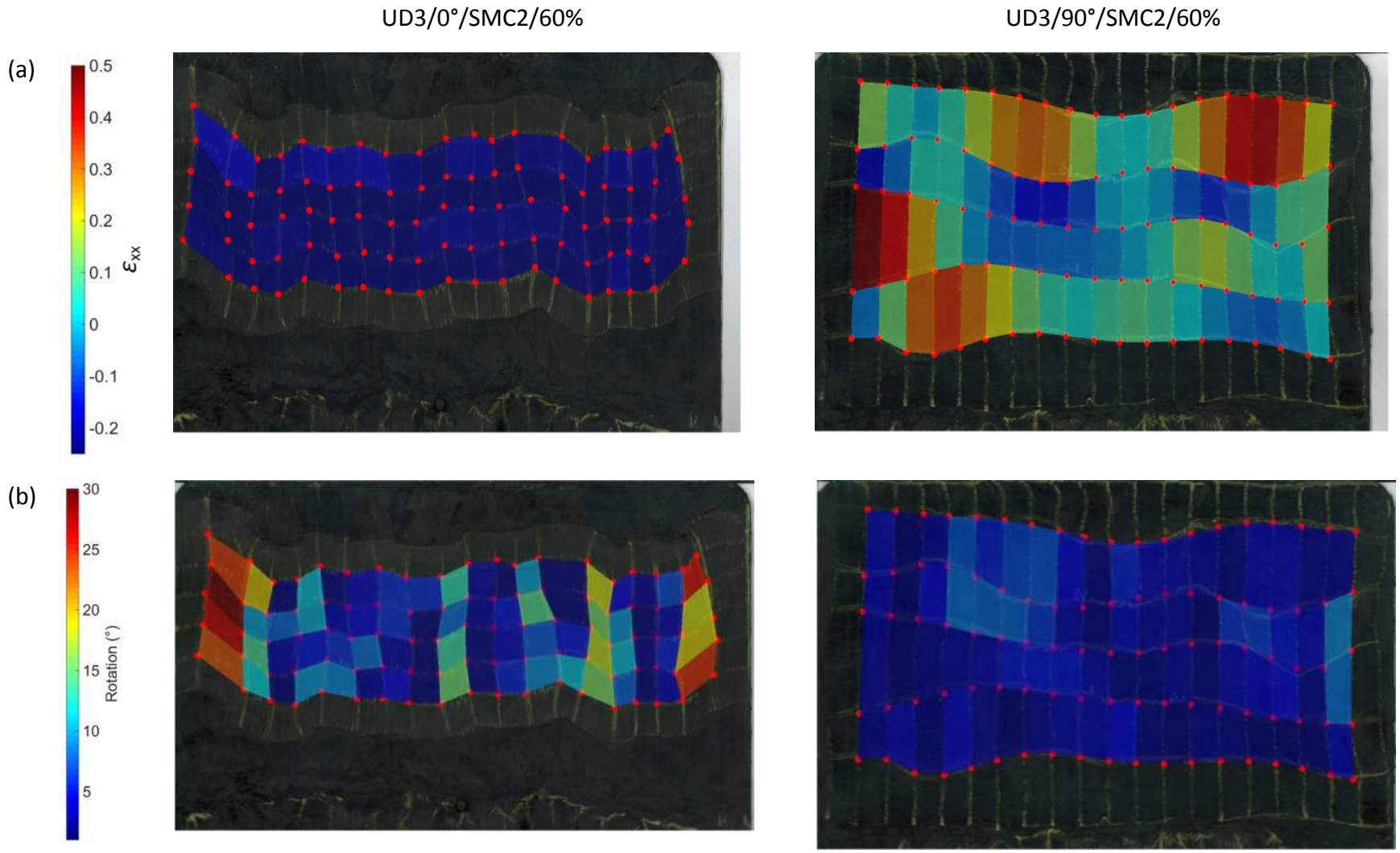

Figure 8: (a) Grid elongation and translation in the x-direction, and (b) element rotation for hybrid plaques UD3/0°/SMC2/60% and UD3/90°/SMC2/60%.

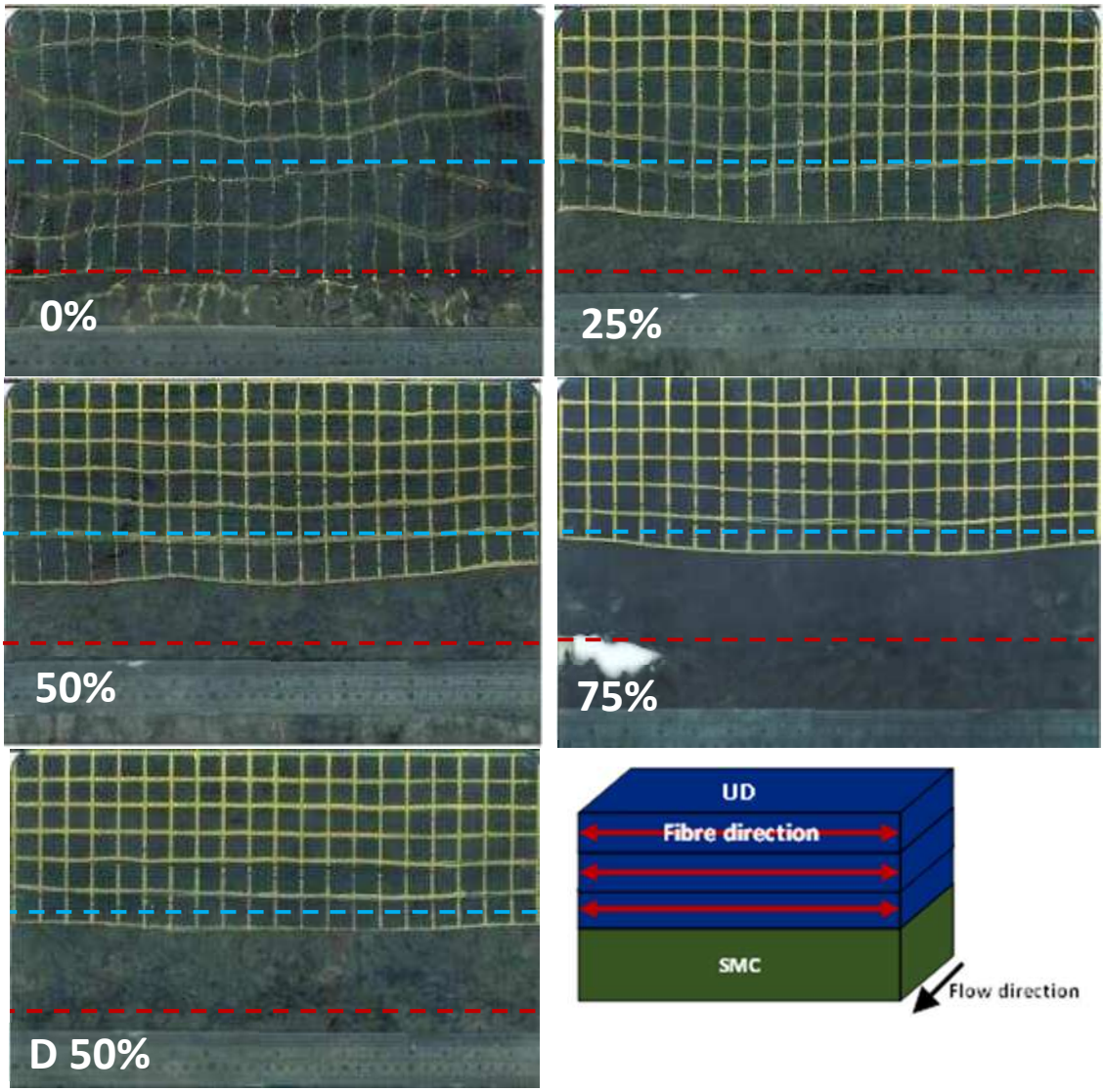

Figure 9: Scanned images of the grids for three plies of staged UD on top of two plies of SMC. Percentages denote staging levels as determined by rheometry, and 'D' denotes ply debulking. Blue dashed line indicates initial charge location, and red dashed line indicates the central symmetry axis (and weld line).

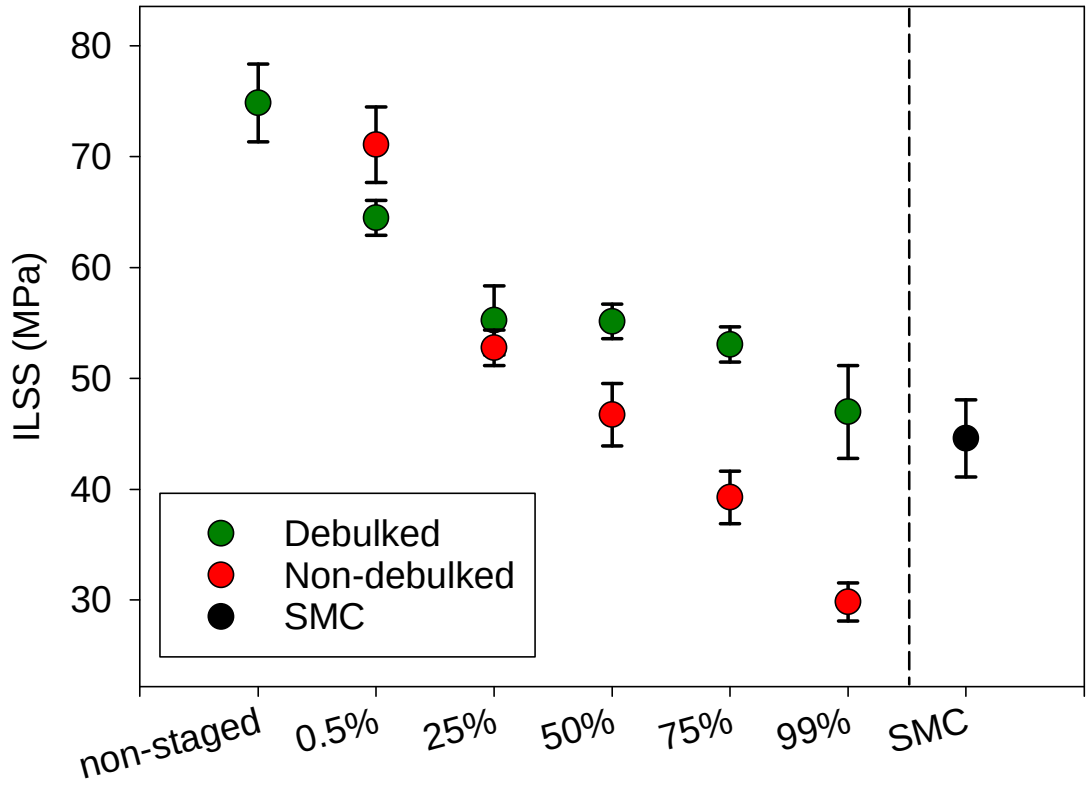

Figure 10: Influence of staging on the ILSS of UD prepreg specimens. ILSS for SMC is included for comparison. Vertical bars indicate 95% confidence interval.

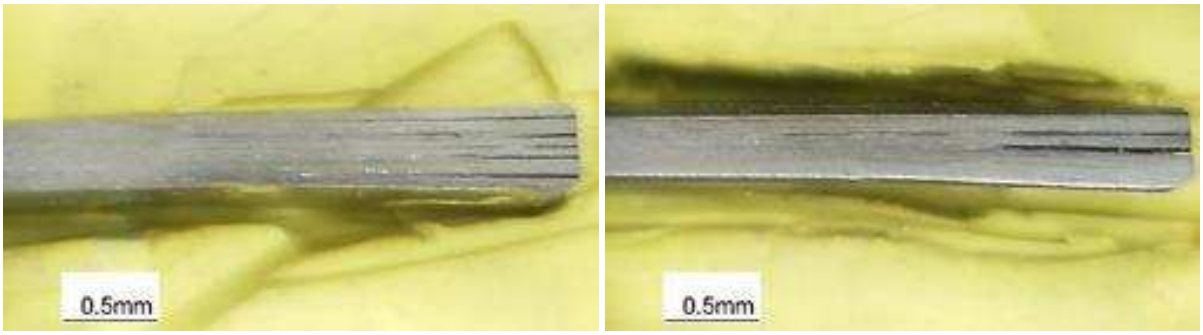

(a) (b)

Figure 11: Edge views of failed ILSS specimens from plaques UD3/90°/SMC2/60% (unstaged) and UD3/90°/SMC2/60%/S75% (75% staged). Three plies of staged UD are at the top of the image in (b).

(a)

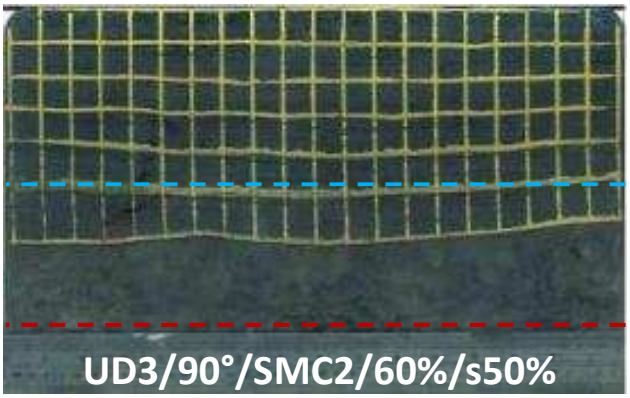

(b)

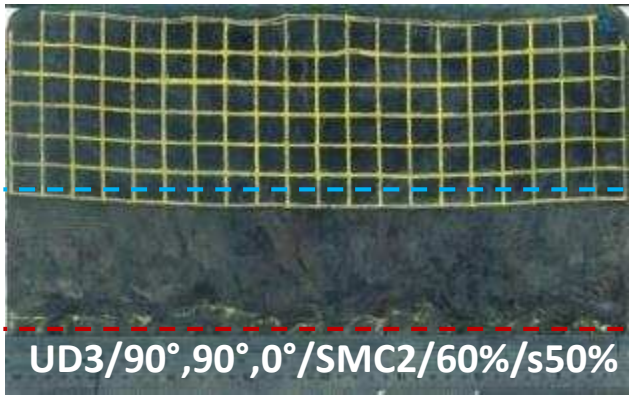

Figure 12: Different charge designs for three plies of 50% staged UD prepreg moulded with 2 plies of SMC. (a) Three UD plies with fibres aligned transverse to flow direction; (b), two UD plies aligned transverse to the flow direction and one UD ply aligned with the flow direction. Blue dashed line indicates initial charge location, and red dashed line indicates the central symmetry axis (and weld line).

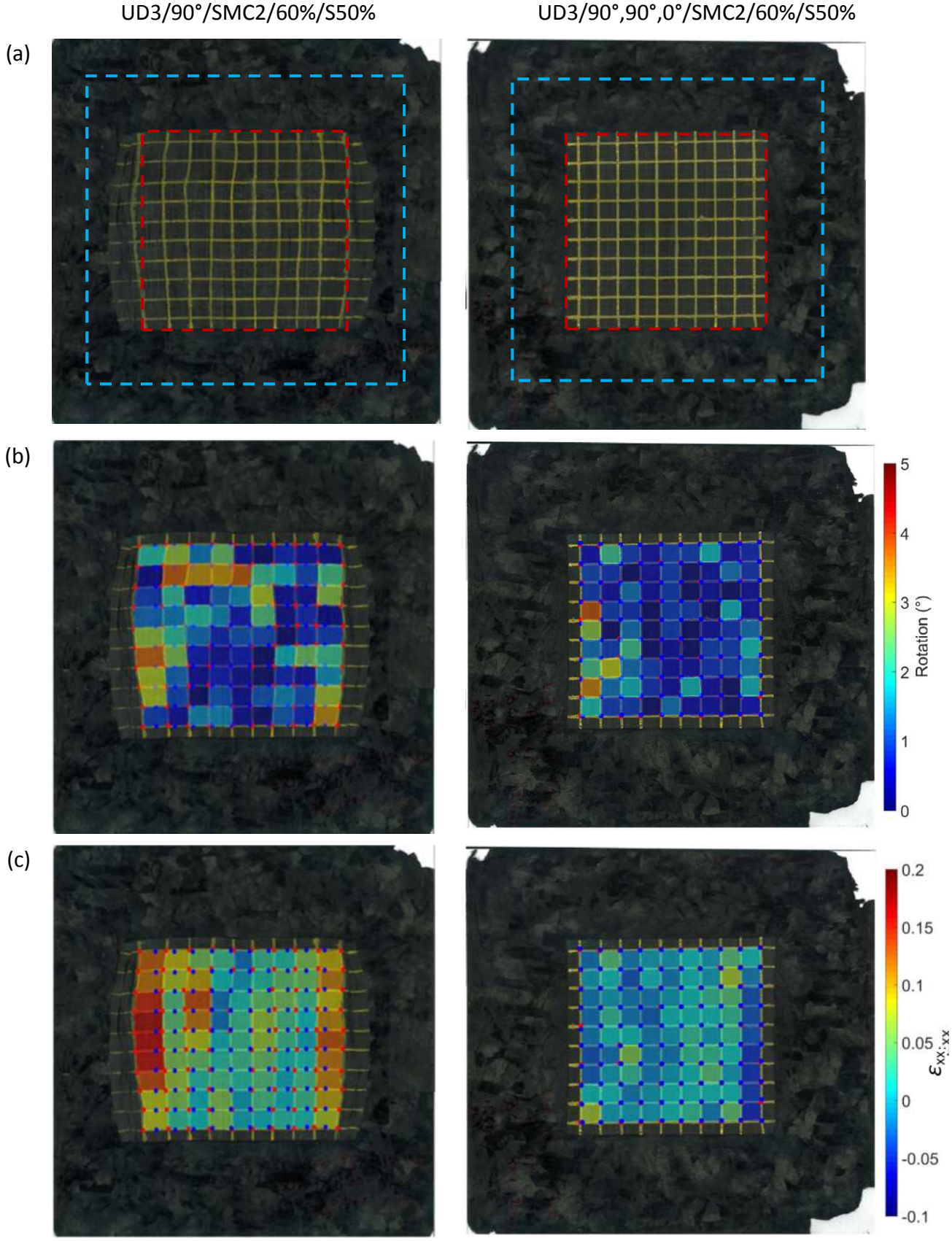

Figure 13: 2D flow study for UD3/90°/SMC2/60%/S50% and UD3/90°,90°,0°/SMC2/60%/S50%. (a) Indicates initial charge position. Red dashed line indicate SMC start point and blue dashed line indicates UD ply start point. (b) Element rotation; (c) element elongation.

9 Tables

Table 1: Plaque construction and moulding details for 1D flow studies

Study # . Plaque #	Designation	Number UD plies	UD ply orientation to flow direction (°)	Number SMC plies	Charge coverage (%)	Staging (%)	Staging Time (Mins)	Debulked (D)
1.1	SMC2/100%			2	100			
1.2	SMC2/60%			2	60			
1.3	UD3/0°/100%	3	0		100			
1.4	UD3/0°/60%	3	0		60			
1.5	UD3/90°/60%	3	90		60			
1.6	UD3/0°/SMC2/60%	3	0	2	60			
1.7	UD3/90°/SMC2/60%	3	90	2	60			
2.1	UD3/90°/SMC2/60%/S0.05%	3	90	2	60	0.05	27	
2.2	UD3/90°/SMC2/60%/S25%	3	90	2	60	25	58	
2.3	UD3/90°/SMC2/60%/S50%	3	90	2	60	50	63	
2.4	UD3/90°/SMC2/60%/S75%	3	90	2	60	75	69	
2.5	UD3/90°/SMC2/60%/S100%	3	90	2	60	100	108	
2.6	UD3/90°/SMC2/60%/S50%/D	3	90	2	60	50	63	D
2.7	UD3/0°/SMC2/60%/S50%	3	0	2	60	50	63	
3.1	UD3/90°,90°,0°/SMC2/60%/S50%	3	90,90,0	2	60	50	63	

Table 2: Distortion measurements taken from the grid analysis for a range of staging levels and different charge designs. Values in brackets indicate the 95% confidence interval. Mechanical properties are presented for the as-moulded fibre volume fractions (non-normalised).

Plaque	Max elong y-dir (%)	Min elong y-dir (%)	Mean elong y-dir (%)	Max elong x-dir (%)	Min elong x-dir (%)	Mean elong x-dir (%)	Max rotation (°)	Min rotation (°)	Mean rotation (°)	Max transl y-dir (mm)	Min transl y-dir (mm)	Mean transl y-dir (mm)	Volume fraction (%)			Flexural Modulus		
													Max	Min	Av	Max	Min	Av
SMC2/100%	-	-	-	-	-	-	-	-	-	-	-	-	58.6	52.8	54.8 (2.0)	34.5	30.8	33.1 (1.2)
SMC2/60% (parallel)	-	-	-	-	-	-	-	-	-	-	-	-	60.0	50.7	53.3 (0.7)	66.7	30.6	45.8 (2.6)
UD3/0°/100%	-	-	-	-	-	-	-	-	-	-	-	-	60.8	58.8	59.8 (0.5)	133.0	126.2	129.1 (2.2)
UD3/0°/60%	3.4	-2.7	0.8 (0.3)	13.3	-6.2	0.5 (1.1)	1.8	0.0	0.5 (0.1)	2.9	-0.5	1.4 (0.2)	73.0	67.2	70.3 (0.5)	161.9	144.9	149.6 (1.5)
UD3/90°/60%	66.5	37.3	49.5 (1.6)	2.2	-4.3	-1.1 (0.2)	6.7	0.0	1.8 (0.4)	52.9	11.7	34.8 (3.0)	77.4	50.2	59.6 (2.1)	123.2	91.1	113.4 (2.4)
UD3/0°/SMC2/60%	19.1	-19.9	-0.1 (2.0)	61.9	-34.5	-1.6 (4.4)	31.7	0.0	8.5 (1.8)	38.2	17.4	31.5 (1.1)	57.9	49.1	54.6 (0.8)	82.9	58.3	72.8 (2.8)
UD3/90°/SMC2/60%	186.1	16.1	76.6 (8.8)	3.3	-17.4	-4.6 (0.9)	8.2	0.1	2.5 (0.5)	64.7	4.0	35.3 (3.8)	59.5	53.3	55.6 (0.6)	83.7	35.4	52.9 (4.9)
UD3/90°/SMC2/60%/S25%	50.8	-2.9	19.9 (3.2)	6.8	-12.4	-0.5 (0.7)	6.3	0.0	1.7 (0.3)	23.6	3.8	11.9 (1.2)	60.0	40.9	54.7 (1.1)	67.4	33.8	51.1 (2.4)
UD3/90°/SMC2/60%/S50%	56.9	-2.5	20.4 (2.7)	10.3	-8.4	-0.3 (0.5)	4.5	0.0	1.2 (0.2)	20.4	4.9	11.0 (1.0)	62.8	46.4	56.0 (1.0)	64.2	33.5	47.8 (2.1)
UD3/90°/SMC2/60%/S75%	33.0	-2.0	10.7 (1.8)	8.1	-8.3	-0.2 (0.7)	3.2	0.0	1.1 (0.2)	8.8	-0.2	3.4 (0.6)	61.4	48.6	55.9 (0.9)	67.5	36.9	49.3 (2.2)
UD3/90°/SMC2/60%/S50%/D	56.4	0.0	15.7 (3.0)	4.9	-5.9	-0.2 (0.5)	3.4	0.0	0.9 (0.2)	10.1	0.0	4.3 (0.7)	61.9	50.9	56.5 (0.8)	78.4	41.7	54.4 (2.6)
UD3/0°/SMC2/60%/S50%	6.8	-9.9	-1.1 (0.7)	12.9	-5.9	0 (1.0)	2.2	0.0	0.7 (0.2)	5.3	2.2	3.7 (0.2)	60.0	48.4	55.1 (0.7)	83.9	44.2	65.7 (2.7)
UD3/90°,90°,0°/SMC2/60%/S50%	6.9	-9.6	0 (0.9)	8.4	-5.6	-0.2 (0.5)	3.4	0.0	1.1 (0.2)	11.4	4.9	9.6 (0.4)	62.2	50.3	56.6 (1.1)	58.3	32.6	44.1 (1.9)